



# HOKKAIDO UNIVERSITY

Title	Metal-insulator transition in $\text{La}_{1-x}\text{Sr}_x\text{TiO}_3$ and $\text{Y}_{1-x}\text{Ca}_x\text{TiO}_3$ investigated by specific-heat measurements
Author(s)	Kumagai, K.; 熊谷, 健一; Suzuki, T. et al.
Citation	PHYSICAL REVIEW B, 48(10), 7636-7642 <a href="https://doi.org/10.1103/PhysRevB.48.7636">https://doi.org/10.1103/PhysRevB.48.7636</a>
Issue Date	1993-09
Doc URL	<a href="https://hdl.handle.net/2115/5893">https://hdl.handle.net/2115/5893</a>
Rights	Copyright © 1993 American Physical Society
Type	journal article
File Information	PRB48-10.pdf



## Metal-insulator transition in $\text{La}_{1-x}\text{Sr}_x\text{TiO}_3$ and $\text{Y}_{1-x}\text{Ca}_x\text{TiO}_3$ investigated by specific-heat measurements

K. Kumagai and T. Suzuki

*Department of Physics, Faculty of Science, Hokkaido University, Sapporo 060, Japan*

Y. Taguchi, Y. Okada, Y. Fujishima, and Y. Tokura

*Department of Physics, Faculty of Science, University of Tokyo, Tokyo 113, Japan*

(Received 1 March 1993)

The carrier-doping (or band-filling) dependence of electronic states has been investigated in the perovskitelike titanate compounds,  $\text{La}_{1-x}\text{Sr}_x\text{TiO}_3$  and  $\text{Y}_{1-x}\text{Ca}_x\text{TiO}_3$ , by measurements of the specific heat. The linear temperature coefficient of the electronic specific heat,  $\gamma$ , is enhanced significantly near the metal-insulator phase-transition boundary, indicating a divergent increase of the effective electron mass due to the strong electronic correlation on approaching the metal-insulator transition boundary. The result is argued in comparison with that of the high- $T_c$  cuprates.

### I. INTRODUCTION

After the discovery of high- $T_c$  cuprate compounds, much effort for understanding the mechanism of high- $T_c$  superconductivity has revealed a number of unusual features in strongly correlated electron systems.<sup>1</sup> The cuprate oxides as well as most of late-3d transition-metal (TM) oxides have been described as charge-transfer-type (CT) insulators with  $d$ - $p$  band gaps, whereas some light transition-metal oxides with strongly correlated  $d$  electrons are known as Mott-Hubbard insulators with  $d$ - $d$  band gaps.<sup>2</sup> For both types of insulating TM oxides, a metallic state can be achieved through band-gap closure or valence (band-filling) control.<sup>3</sup> The change of the Cu valence of cuprates, for example, provides a transitional nature from the antiferromagnetic insulating to metallic state through the high- $T_c$  superconducting state.<sup>1</sup>

The Mott-insulator-metal phase transition is investigated mostly with the Hubbard model.<sup>4</sup> This model is also regarded as one of the relevant models for high- $T_c$  superconductivity. However, a rigorous prediction based on the Hubbard model has not been given as to how the system evolves from a paramagnetic metal to an antiferromagnetic insulator as  $U/W$  is changed ( $U$ : intra-atomic Coulomb energy;  $W$ : one-electron bandwidth) or as the band filling is changed. Thus, extensive investigations from both experimental and theoretical viewpoints on an evolution of the electronic structure with carrier doping will be currently required to shed light on the problem of highly correlated  $d$ -electron systems. Furthermore, the study of the doped Mott-Hubbard compounds may bring about information complementary to that of the high- $T_c$  cuprates which are assigned to the doped CT insulators.

Perovskite oxides  $R_{1-x}A_x\text{TiO}_3$  recently have been of renewed interest because of their physical and chemical properties changing with the filling of  $d$  electrons.<sup>5-13</sup> The formal valence of titanium can be changed from  $+3(3d^1)$  to  $+4(3d^0)$  by alloying the  $R$ -site cations with

trivalent rare-earth ions (Y, La) and the  $A$ -site cations with divalent alkali-earth ions (Ca, Sr). One of the end compounds of  $\text{SrTiO}_3$  ( $\text{CaTiO}_3$ ) has no  $d$  electron and is assigned to a band insulator.<sup>14</sup> The other end insulating compound  $\text{LaTiO}_3$  ( $\text{YTiO}_3$ ) has been reported to be in a magnetically ordered state with a Mott-Hubbard gap at low temperature.<sup>5,6,7</sup>

In this paper, we report on changes of the electronic state induced by carrier doping (or band filling) for  $\text{La}_{1-x}\text{Sr}_x\text{TiO}_3$  and  $\text{Y}_{1-x}\text{Ca}_x\text{TiO}_3$  by measurements of low-temperature heat capacity. A critical behavior of the electronic specific heat observed near the metal-insulator boundary is of particular interest for understanding the low-energy electronic state in the doped Mott-Hubbard systems with strong electron correlation. We discuss also a clear difference in the doping dependences of the electronic states between the high- $T_c$  cuprate and the doped titanate systems.

### II. EXPERIMENT

Samples were melt grown by a floating-zone method in a reduced or inert-gas atmosphere and the details have been reported elsewhere.<sup>12,13,15</sup> Careful attention to the oxygen stoichiometry was paid to in the synthesis of the samples close to  $x=0$ . Thermogravimetric analysis showed that the off stoichiometry of oxygen in the samples was fairly small ( $\delta < 0.01$  in the formula of  $\text{LaTiO}_{3+\delta}$  and  $\delta < 0.03$  for  $\text{YTiO}_{3+\delta}$ ). X-ray-diffraction patterns indicated that all the samples were of the single phase of the orthorhombically distorted perovskite-type ( $\text{GdFeO}_3$ -type). The temperature dependences of the electrical resistivity show that the metal-insulator boundary is near  $x=0$  for the La-Sr system<sup>12,13</sup> and near  $x=0.4$  for the Y-Ca system.<sup>15</sup> The electronic and magnetic phase diagram for the  $R_{1-x}A_x\text{TiO}_3$  system<sup>16</sup> is shown schematically in Fig. 1. In the metallic region, the magnetic susceptibility is nearly temperature independent, typical of the Pauli paramagnetism and is free from im-

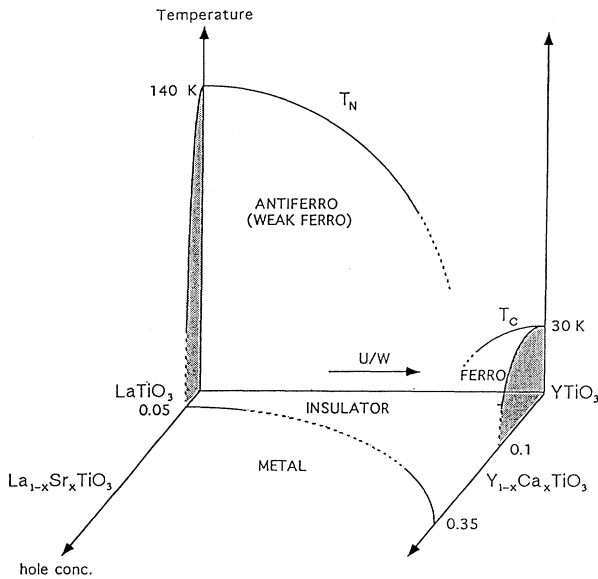


FIG. 1. Electronic and magnetic phase diagram in  $R_{1-x}A_x\text{TiO}_3$  ( $R=\text{La}, \text{Y}$  and  $A=\text{Sr}, \text{Ca}$ ) from Ref. 16.

purities with localized moments.<sup>13,15</sup> The heat capacity was measured by a conventional adiabatic heat-pulse method with the use of calibrated Ge thermometers down to 1 K.

### III. RESULTS AND DISCUSSION

#### A. $\text{La}_{1-x}\text{Sr}_x\text{TiO}_3$ system

Figure 2 shows heat capacity divided by temperature ( $C/T$ ) as a function of the square of the temperature for  $\text{La}_{1-x}\text{Sr}_x\text{TiO}_3$ .<sup>17</sup> The heat capacity at low temperature is in good agreement with the relation,  $C = \gamma T + \beta T^3$ , where the first term is ascribed to the electronic contribution with  $\gamma = 1/3\pi^2 k_B^2 N(0)$  and the second term to the lattice contribution with  $12/5\pi^4 k_B N(1/\Theta_D)^3$ . Here  $N(0)$  is the renormalized electronic density of states at the Fermi level,  $N$  is the number of atoms in a unit cell, and  $\Theta_D$  is the Debye temperature. Neither upturn nor downturn behavior for the  $C/T$  vs  $T^2$  plot is observed down to

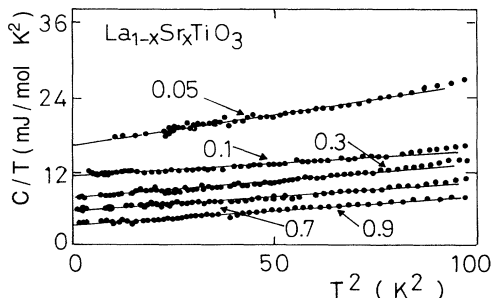


FIG. 2.  $C/T$  as a function of  $T^2$  for  $\text{La}_{1-x}\text{Sr}_x\text{TiO}_3$ .

1 K, which enables us to determine the  $\gamma$  value unambiguously. The Debye temperature obtained is 450–550 K and does not depend very much on the composition.

Figure 3 shows the band-filling ( $n = 1 - x$ ) dependence of the  $\gamma$  values of  $\text{La}_{1-x}\text{Sr}_x\text{TiO}_3$ . Here, the  $\gamma$  values are determined by the least-squares fitting in the low-temperature region ( $T < 10$  K). For a parabolic band,  $N(0)$  is given by  $N(0) = (4\pi/h^3)(2m^*)^{3/2}E_F^{1/2}$ , and  $E_F = (h^2/2m^*)(3\pi^2n_0)^{2/3}$ . Thus,  $\gamma \propto m^*n_0^{1/3}$ , where  $m^*$  is the effective electron mass and  $n_0$  is the carrier density. A solid line in Fig. 3 represents the band-filling ( $n = 1 - x$ ) dependence of the  $\gamma$  value ( $\propto n^{1/3}$ ) for the noninteracting electron case. Here a bare value for a free-electron model is assumed to be 2.8 mJ/mol K<sup>2</sup> for  $n = 0.1$  ( $x = 0.9$ ), which is a value expected for the reasonable bandwidth ( $\sim 1$  eV). In the low- $n$  (high- $x$ ) region, the  $n$  dependence of  $\gamma$  seems to obey this relation well, implying that the picture of band filling in the band insulator may be valid, as the 3d band is filled up from the band bottom with increasing  $n$  from  $n = 0$  (or decreasing  $x$  from  $x = 1$ ). On the contrary, on approaching the metal-insulator phase boundary, i.e.,  $x = 0$  ( $n = 1$ ) for  $\text{La}_{1-x}\text{Sr}_x\text{TiO}_3$ , the  $\gamma$  values are largely enhanced compared to the values expected for the simple rigid-band picture with band filling.

As the Hall coefficient varies linearly as a function of  $n$  ( $n = 1 - x$ ) up to at least  $n = 0.95$  for  $\text{La}_{1-x}\text{Sr}_x\text{TiO}_3$ ,<sup>12</sup> the 3d band filling gives a precise measure of the carrier density even in the composition region close to the insulating end ( $x \sim 0$ ). Therefore, the divergent increase of the  $\gamma$  value shows that the effective  $d$ -electron mass at the Fermi level is critically enhanced on approaching the metal-insulator phase boundary. The large enhancements of specific heat and magnetic susceptibility have been re-

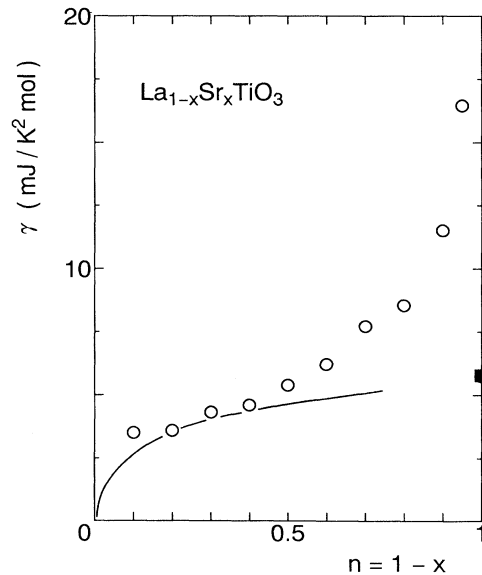


FIG. 3. Filling ( $n = 1 - x$ ) dependence of  $\gamma$  ( $\circ$ ) for  $\text{La}_{1-x}\text{Sr}_x\text{TiO}_3$ . The symbol ( $\blacksquare$ ) represents the  $\gamma$  value obtained for the antiferromagnetic  $\text{LaTiO}_3$ . The solid line shows the band-filling,  $n = (1 - x)^{1/3}$ , dependence of  $\gamma$ .

ported in the vanadium oxide family,  $V_nO_{2n-1}$ ,<sup>18</sup> although detailed carrier-number dependence of the enhanced effective mass has not been clarified in the previous studies.

The end member compound,  $\text{LaTiO}_3$  undergoes an antiferromagnetic transition around  $T_N=120\text{--}145\text{ K}$ .<sup>5</sup> Some experiments on  $\text{LaTiO}_3$  have indicated that electrical and magnetic properties are highly sensitive to oxygen stoichiometry.<sup>9</sup> Because of an uncalibrated Ge thermometer above 100 K, we did not measure the heat capacity of  $\text{LaTiO}_3$  in the high-temperature region across a magnetic transition temperature, but we obtained the low-temperature heat capacity in the magnetically ordered state, which disclosed a much reduced  $\gamma$  value ( $\sim 5\text{ mJ/mol K}^2$ ). As the Mott-Hubbard antiferromagnet with the exact  $n=1$  filling is expected to have no carriers because of the existence of the Mott-Hubbard gap ( $\sim 0.1\text{ eV}$ ),<sup>12</sup> the finite  $\gamma$  value of the present  $\text{LaTiO}_3$  may be attributed to a contribution from residual carriers due to the unavoidable off-stoichiometry of oxygen in the present sample.

### B. $\text{Y}_{1-x}\text{Ca}_x\text{TiO}_3$ system

Within the family of  $\text{RTiO}_3$  ( $R$  is any of the rare-earth ions from La to Lu), the electrical and magnetic properties depend systematically on the ionic radius of  $R^{3+}$ .<sup>19</sup> The  $\text{RTiO}_3$  crystal can be viewed as an orthorhombically distorted perovskite structure (so-called  $\text{GdFeO}_3$ -type structure) where the  $\text{TiO}_8$  octahedron tilts alternatively. The ionic radius of Y (and Ca) is smaller than that of La(Sr), which affects the one-electron bandwidth due to a larger deviation of the Ti-O-Ti bond angle from  $180^\circ$ .<sup>19</sup> Therefore, the electronic correlation strength  $U/W$  of the Y-Ca system is large compared to that of the La-Sr system. In fact, the measurements of the electrical resistivity show that the insulating behavior appears near  $x=0.4$  ( $n=0.6$ ), which is far from the  $n=1$  filling.<sup>15</sup> In contrast to the antiferromagnetic ground state of the insulating  $\text{LaTiO}_3$ ,  $\text{YTiO}_3$ , with a relatively narrower  $3d$  bandwidth, is a ferromagnetic insulator with a Mott-Hubbard gap of  $\sim 1\text{ eV}$ .<sup>15</sup> The ferromagnetic ground state may arise from the orbital degeneracy in the  $3d$  states, although details of the microscopic origin are left to be clarified. The magnetic and electronic phase diagram described here is depicted schematically in Fig. 1. Comparison of transitional behavior across the electronic evolution in  $\text{La}_{1-x}\text{Sr}_x\text{TiO}_3$  and  $\text{Y}_{1-x}\text{Ca}_x\text{TiO}_3$  also will be interesting.

The heat capacity of  $\text{Y}_{1-x}\text{Ca}_x\text{TiO}_3$  is shown in Fig. 4. The heat capacity obeys the relation  $C/T=\gamma+\beta T^2$  for the metallic region of  $x>0.5$ . As no upturn or downturn behavior for the  $C/T$  vs  $T^2$  plot are observed down to near 1 K in the metallic state, the  $\gamma$  values can be determined unambiguously in this case, similar to the metallic  $\text{La}_{1-x}\text{Sr}_x\text{TiO}_3$  case. In the insulating region of  $x<0.4$ , however, the heat capacity is largely enhanced and does not obey the linear relation  $C/T$  vs  $T^2$  plot as seen in Fig. 4(b).

In Fig. 5, we show the  $x$  dependences of  $\gamma$  obtained in the metallic region of  $\text{Y}_{1-x}\text{Ca}_x\text{TiO}_3$  as well as

$\text{La}_{1-x}\text{Sr}_x\text{TiO}_3$ . Here the  $\gamma$  values are determined by the least-squares fitting of the experimental data obtained by the relation of  $C/T=\gamma+\beta T^2$  in the low-temperature region ( $T<10\text{ K}$ ). The  $x$  dependences of the Pauli paramagnetic susceptibility  $\chi$  of both systems<sup>12,13</sup> are also shown in Fig. 5. It should be noted that the doping (or filling) dependences of the electronic specific heat show quite a parallel behavior with the magnetic susceptibility in the metallic region for the both systems. Magnetic susceptibility in the metallic region shows a nearly temperature-independent behavior which is typical of the Pauli paramagnetic susceptibility.<sup>12,13</sup> As  $\chi_{\text{Pauli}}$  is proportional to the density of states at the Fermi level, i.e.,  $\chi_{\text{Pauli}}=2\mu_B^2 N(0)$ , the observed parallel change of  $\gamma$  and  $\chi_{\text{Pauli}}$  with  $x$  demonstrates clearly a critical enhancement of the effective electron mass as the metal-insulator transition boundary is approached. The Wilson ratio  $\chi/\gamma$  in units of  $3\mu_B^2/\pi^2 k_B \mu_B^2$  is nearly constant ( $\sim 2$ ) over the whole range of  $x$ . This result indicates the absence of the Stoner enhancement even near the metal-insulator boundary. This is in contrast to the system with the predominant paramagnon interactions, where  $\chi$  is exchange enhanced and  $\gamma$  is mass enhanced so that the Wilson ratio diverges as the onset of itinerant ferromagnetism is approached.<sup>20</sup>

The present study on the critical enhancement of effective mass may suggest the importance of the single-site electron correlation in driving the metal-insulator transition in accord with the Brinkmann-Rice picture,<sup>21</sup> which indicates that the effective mass relevant to both the electronic heat capacity and the spin susceptibility diverges as  $m^*/m=[1-(U/U_0)^2]^{-1}$ , where  $U_0$  is the critical value for the intra-atomic Coulomb interaction.

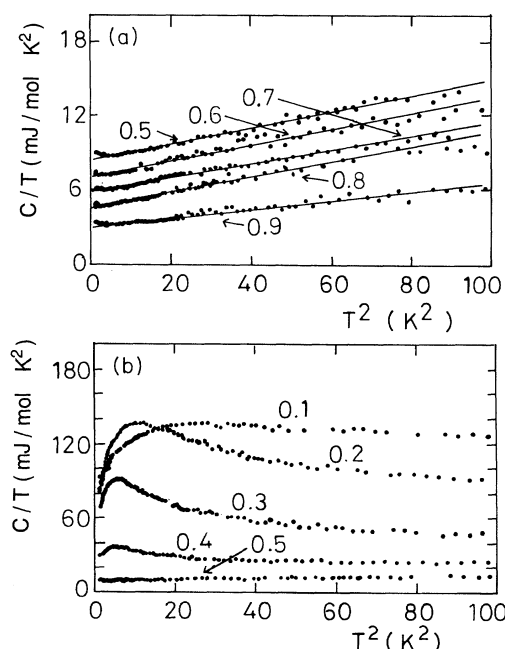


FIG. 4.  $C/T$  as a function of  $T^2$  for  $\text{Y}_{1-x}\text{Ca}_x\text{TiO}_3$ . (a) for the metallic region ( $x \geq 0.5$ ), (b) for the barely metallic or insulating region ( $x \leq 0.5$ ). The result for  $x=0.5$  is shown in both figures.

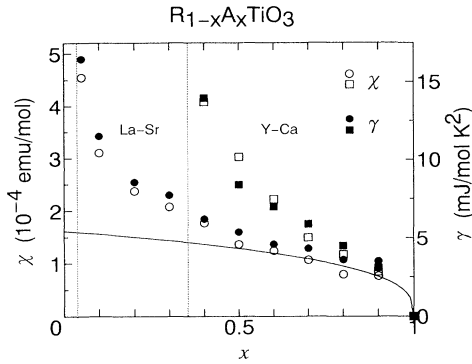


FIG. 5.  $x$  dependences of  $\gamma$  (●, ■) and the Pauli paramagnetic susceptibility  $\chi$  (○, □) in the metallic region of  $\text{La}_{1-x}\text{Sr}_x\text{TiO}_3$  and  $\text{Y}_{1-x}\text{Ca}_x\text{TiO}_3$ . The vertical dotted lines show the metal-insulator phase boundary determined by electrical resistivity (Refs. 13 and 15) and the solid line shows the  $(1-x)^{1/3}$  dependence of  $\gamma$ .

In terms of the Fermi-liquid picture extended to the barely metallic region close to  $x=0$ , the enlarged  $\gamma$  and  $\chi$  are ascribed to the formation of heavy-electron liquid by strong correlation. In accord with this picture, the ratio of the coefficient of the  $T^2$  dependence of electrical resistivity and the  $\gamma$  value for  $\text{La}_{1-x}\text{Sr}_x\text{TiO}_3$  in the vicinity of the metal-insulator phase boundary was found to agree quite well with the universal value<sup>12</sup> reported for the heavy-fermion systems.<sup>22</sup>

In order to see the detail of the electronic contribution for  $x \leq 0.4$  (insulating region) in  $\text{Y}_{1-x}\text{Ca}_x\text{TiO}_3$ , we show the electronic specific heat by subtracting the lattice contribution obtained for  $x=0.9$  in Fig. 6. The electronic specific heat changes significantly with temperature, implying that the coefficient of the electronic specific heat  $\gamma$  is temperature dependent as opposed to that in a simple metallic picture. The electronic heat capacity for  $x=0.2-0.4$  seems to increase logarithmically and then decreases with decreasing temperature. The characteristic temperature  $T_0$ , giving the maximum heat capacity, increases gradually with decreasing  $x$ , i.e.,  $T_0=2, 2.5, 3.5,$  and  $5.5$  for  $x=0.4, 0.3, 0.2,$  and  $0.1$ , respectively. The maximum electronic contribution is as large as  $140 \text{ mJ/mol K}^2$  for  $x=0.2-0.1$ . This value is exceptionally

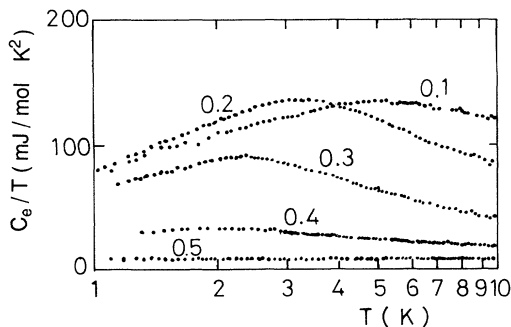


FIG. 6. Electronic heat capacity divided by temperature as a function of  $\log T$  in the insulating region of  $\text{Y}_{1-x}\text{Ca}_x\text{TiO}_3$ . The lattice contribution is subtracted by using  $\beta=0.065$ , obtained for the  $x=0.1$  data.

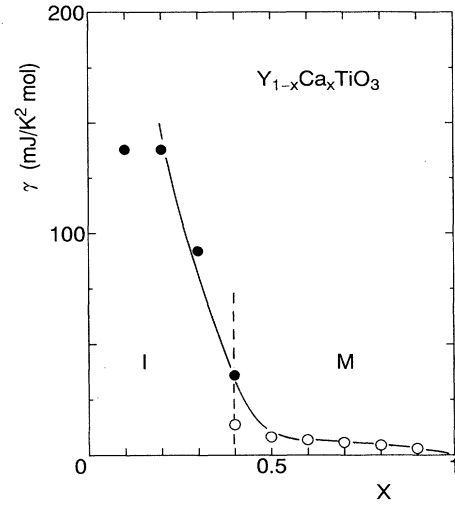


FIG. 7.  $x$  dependence of  $\gamma$  value (●) in the insulating region ( $x \leq 0.4$ ) of  $\text{Y}_{1-x}\text{Ca}_x\text{TiO}_3$ . The maximum values of the electronic contribution of  $C_e/T$  are plotted. The  $\gamma$  values in the metallic region of  $x \geq 0.4$  (of which detail is shown in Fig. 5) are also shown. The  $\gamma$  value (○) for  $x=0.4$  is determined by fitting to the  $C/T = \gamma + \beta T^2$  relation in the temperature range of  $100 < T^2 < 500$  and use of the same  $\beta$  value obtained for  $x=0.5$ .

large for the  $3d$  electron systems.<sup>18</sup>

The maximum  $T$  linear coefficient  $\gamma$  of the electronic heat capacity obtained from the  $C_e/T$  plot (Fig. 6) is also shown in Fig. 7. This  $\gamma$  value is enhanced significantly with  $x$  for  $x \leq 0.4$ , where the electrical resistivity shows an apparent insulating (or semiconducting) behavior in its temperature dependence.<sup>15</sup> Therefore, the metal-insulator phase transition near  $x=0.4$ , which is far from the  $n=1$  filling condition in  $\text{Y}_{1-x}\text{Ca}_x\text{TiO}_3$ , may be attributed to the large enhancement of the renormalized electron mass due to strong electron correlation. As the long-range spin order seems to vanish for  $x > 0.1$  in  $\text{Y}_{1-x}\text{Ca}_x\text{TiO}_3$ , the metal-insulator transition near  $x=0.4$  in  $\text{Y}_{1-x}\text{Ca}_x\text{TiO}_3$  is not simply related to the presence of the magnetically ordered phase. The nonmetallic behavior in electrical resistivity for  $x < 0.4$  may be characterized by a combined effect of the electron correlation and random potential arising from the ionic Y and Ca mixture. When the enhanced mass exceeds some critical value, the localization of the carrier appears.

We would like to stress again that the barely metallic behavior for  $x < 0.4$  in  $\text{Y}_{1-x}\text{Ca}_x\text{TiO}_3$  is not characterized by the decrease of carrier density but by the increase of the effective mass of carriers. Namely, the electrical conductivity of the doped Mott insulator, given by  $\sigma \propto n/m^*$ , becomes vanishingly small as  $m^*$  tends to diverge, while  $n$  is not changed as much. Such a critical filling dependence of  $m^*$  has been predicted by the recent theoretical investigations of the one-,<sup>23</sup> two-,<sup>24</sup> and infinite-<sup>25</sup> dimensional Hubbard models.

### C. Ferromagnetic transition $\text{YTiO}_3$

As described in Sec. III B a ferromagnetic order of  $3d$  electrons of Ti ions has been observed in the vicinity of

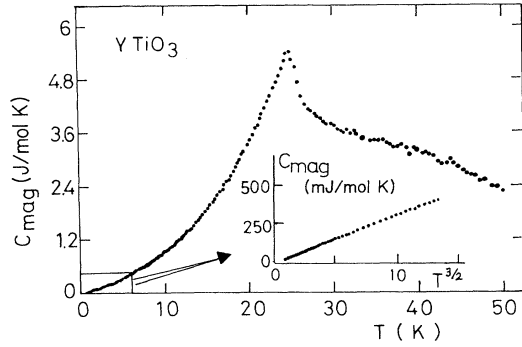


FIG. 8. Magnetic heat capacity of  $\text{YTiO}_3$  as a function of temperature. The lattice contribution is subtracted by using the result of  $x=0.9$ . The inset shows the detail of the low-temperature part as a function of  $T^{3/2}$ .

the  $n=1$  filling condition of  $\text{Y}_{1-x}\text{Ca}_x\text{TiO}_3$ .<sup>6,7</sup> Figure 8 shows the magnetic heat capacity of  $\text{YTiO}_3$  as a function of temperature. Here the magnetic heat capacity is obtained by subtracting the lattice contribution, using the result for  $x=0.9$ . A steep peak is observed at 25 K which coincides with the transition temperature for the long-range magnetic ordering of Ti spins. The magnetic entropy at  $T_c$  is 60% of that expected for the spin freedom of  $S=\frac{1}{2}$ . Some amount of the magnetic contribution above  $T_c$  exists due to short-range spin fluctuations in the present system. As the magnetic nature may be sensitive to slight off stoichiometry of the sample,<sup>13</sup> details for the magnetic contributions above  $T_c$  will be required for further discussion.

It should be noted that the low-temperature part of the magnetic heat capacity obeys quite well the  $T^{3/2}$  relation, which is expected for the contribution from the spin-wave excitations in the ferromagnetic case. According to the simple spin-wave approximation for the three-dimensional ferromagnetic case, the magnetic heat capacity is given by<sup>26</sup>

$$C_{\text{spin wave}} = \frac{15}{4} R \xi\left(\frac{5}{2}\right) (kT/8\pi JS)^{3/2} T^{3/2},$$

where  $\xi$  is Riemann's zeta function and  $\xi\left(\frac{5}{2}\right)$  is 1.341,  $R$  is the gas constant,  $S$  is the spin of an ion, and the exchange constant  $J$  is given by the dispersion relation of  $h\omega_q = 2JSq^2$  for small  $q$ . The coefficient of the  $T^{3/2}$  term was found to be  $3.73 \times 10^{-3}$  (in units of  $R$ ) from a root-mean-square fitting. Thus, a value for the exchange constant  $J$  was found to be  $3.32 \times 10^{-4}$  eV. This value seems to be a reasonable one in comparison with those reported in typical ferromagnets.<sup>27</sup> The ratio  $kT_c/J$  is 6.5, which may be compared with a value for a simple single-exchange Heisenberg model.<sup>28</sup> We may conclude from a thermodynamic viewpoint that the magnetic order is a ferromagnetic one in accord with the magnetization measurements.<sup>15</sup>

#### D. Comparison with the result in $\text{La}_{2-x}\text{Sr}_x\text{CuO}_4$

It is interesting to compare the carrier-doping effect on the evolution of electronic states between cuprates with

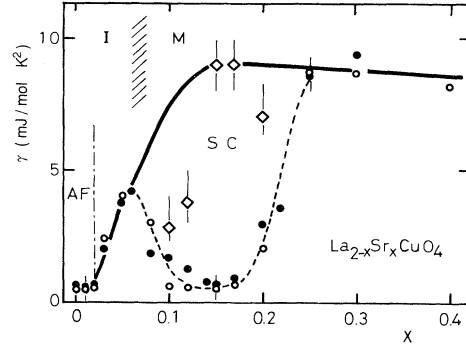


FIG. 9.  $x$  dependence of  $\gamma$  for  $\text{La}_{2-x}\text{Sr}_x\text{CuO}_4$ . The solid circle is obtained from the low-temperature fitting ( $T < 0.5$  K) with  $C = \gamma T + A/T^2$  (Refs. 30 and 31), where the second term is the nuclear Schottky contribution. The open circle is obtained by the fitting to  $C/T = \gamma + \beta T^2$  in the high-temperature range ( $2 < T < 10$  K) (Ref. 29). The open square is obtained from the jump of heat capacity at  $T_c$  and the BCS relation of  $\Delta C/\gamma T_c = 1.43$ .

the charge-transfer gap and titanates with the Mott-Hubbard gap. The hole-doping dependence of  $\gamma$  in the doped Mott system is quite in contrast to that obtained in high- $T_c$  cuprates.<sup>29-31</sup> For a clear demonstration of the situation, we show the  $x$  dependence of  $\gamma$  in  $\text{La}_{2-x}\text{Sr}_x\text{CuO}_4$  in Fig. 9. (The figure is redrawn from the ones reported originally in Refs. 29 and 31.) From the electrical resistivity measurement, the electronic state is found to be insulating for  $x < 0.06$  and metallic for  $x > 0.06$  in  $\text{La}_{2-x}\text{Sr}_x\text{CuO}_4$ .<sup>32</sup>

In the superconducting region ( $0.06 < x < 0.25$ ), the  $\gamma$  value at low temperatures becomes vanishingly small due to the opening of the superconducting energy gap. In this case, the coefficient of the electronic specific heat of the normal state,  $\gamma_n$ , has been estimated from the heat-capacity jump  $\Delta C$  at the superconducting transition temperature  $T_c$ .<sup>31</sup> These estimated  $\gamma_n$  values of the normal state are shown in Fig. 9 with the open square, assuming the BCS-type relation,  $\Delta C/\gamma_n T_c = 1.43$ . The  $\gamma$  value is nearly zero (or less than  $1 \text{ mJ/mol K}^2$ ) for  $x < 0.02$ , where the long-range antiferromagnetic order exists.  $\gamma_n$  increases gradually with increasing  $x$  from  $x=0.02$  to 0.15 across the metal-insulator boundary. In other words, the decrease of  $\gamma$  seems to be accompanied with decreasing carrier doping for  $x < 0.15$ . Signs of the divergent behavior of  $\gamma$  do not appear around  $x=0.06$ . The estimated  $\gamma_n$  value ( $9 \text{ mJ/mol K}^2$ ) near  $x=0.15$  becomes almost comparable to the  $\gamma$  value in the normal metallic region of  $x > 0.3$ . The gradual decreases of  $\gamma_n$  with decreasing  $x$  from the metallic region have been similarly observed in the electron-doped cuprates of  $\text{Pr}_{2-x}\text{Ce}_x\text{CuO}_4$ .<sup>33,34</sup>

Thus, it may be a characteristic feature in the doped cuprates that the divergent behavior in the mass enhancement of the correlated electrons is absent across the metal-insulator boundary. The gradual decrease of the electronic specific heat toward the metal-insulator bound-

ary in the doped cuprates is rather surprising, considering that the electronic correlation should increase substantially on approaching the insulating state.<sup>35</sup> This result in the cuprates is in striking contrast to those of the doped titanates presented here.

#### IV. CONCLUSION

The band-filling-induced change of electronic states have been investigated for the perovskite titanate compounds,  $\text{La}_{1-x}\text{Sr}_x\text{TiO}_3$  and  $\text{Y}_{1-x}\text{Ca}_x\text{TiO}_3$ . From the  $C/T$  vs  $T_2$  plot without any upturn or downturn behavior down to 1 K, the  $\gamma$  values in the metallic region have been determined unambiguously in both systems. Together with the results of the magnetic susceptibility and Hall effect,<sup>12,13,15</sup> the present study on the electronic specific heat indicates clearly that the effective mass of  $3d$  electrons in the doped Mott-Hubbard system is enhanced critically (or divergently) on approaching the metal-insulator phase boundary. Quite a parallel behavior of  $\gamma$  and the Pauli paramagnetic susceptibility  $\chi$  with carrier doping (or band filling) in the metallic region indicates that the heavy-electron liquid state is formed through the development of local spin fluctuations with a dominant single-site correlation.

For the rather strongly correlated system  $\text{Y}_{1-x}\text{Ca}_x\text{TiO}_3$ , the electronic heat capacity is extremely enhanced and its temperature dependence is not simply

characteristic of metallic behavior for  $x < 0.4$  ( $n > 0.6$ ). The significantly enhanced electron mass as well as the random potential, which arise mainly from the ionic Y-Ca mixture, causes the localization of the electronic state at the composition far from the  $n=1$  filling condition. The metal-insulator transition in the doped Mott-Hubbard system is not driven by the decrease of carrier density but by the divergent enhancement of the renormalized electron mass due to electron correlations.

Finally, we would like to remark that the carrier-doping effect on the electronic specific heat is clearly different between the cuprate (charge-transfer-type) and the titanate (Mott-Hubbard-type) compounds. The metal-insulator transition without a notable enhancement of electron mass with carrier doping in high- $T_c$  cuprates may be characterized by a decrease in the carrier density,<sup>32</sup> which is in contrast to the present titanate case. These findings on the distinctly different types of evolution of the electronic structures in these highly correlated systems may be crucial for understanding the mechanism of high- $T_c$  superconductivity.

#### ACKNOWLEDGMENTS

The authors are grateful to M. Imada for enlightening discussions. This work was supported by a Grant-in-Aid for Scientific Research on Priority Areas given by the Ministry of Education, Science and Culture of Japan.

<sup>1</sup>For instance, see *Proceedings of M<sup>2</sup>S - HTSC III (Kanazawa)* [Physica C **185-189**, (1992)].

<sup>2</sup>J. Zaanen, G. A. Sawatzky, and J. W. Allen, Phys. Rev. Lett. **55**, 418 (1985).

<sup>3</sup>A. Fujimori, J. Phys. Chem. Solids **53**, 1595 (1992).

<sup>4</sup>J. Hubbard, Proc. Phys. Soc. London A **276**, 238 (1963); **277**, 237 (1964); **281**, 401 (1964).

<sup>5</sup>D. A. MacLean, K. Seto, and J. E. Greedan, J. Solid State Chem. **40**, 241 (1981).

<sup>6</sup>J. D. Garret, J. E. Greedan, and D. A. MacLean, Mater. Res. Bull. **16**, 145 (1981).

<sup>7</sup>J. P. Goral, J. E. Greedan, and D. A. MacLean, J. Solid State Chem. **43**, 244 (1982).

<sup>8</sup>Y. Maeno, S. Awaji, H. Mastumoto, and T. Fujita, Physica B **165-166**, 1185 (1990).

<sup>9</sup>F. Lichtenberg, D. Widmer, J. G. Bednorz, T. Williams, and A. Reller, Z. Phys. B **82**, 211 (1991).

<sup>10</sup>Y. Fujishima, Y. Tokura, T. Arima, and S. Uchida, Physica C **185-189**, 1001 (1991).

<sup>11</sup>D. A. Crandles, T. Timusk, and J. E. Greedan, Phys. Rev. B **44**, 13 250 (1991).

<sup>12</sup>Y. Fujishima, Y. Tokura, T. Arima, and S. Uchida, Phys. Rev. B **46**, 11 167 (1992).

<sup>13</sup>Y. Tokura, Y. Taguchi, Y. Okada, Y. Fujishima, T. Arima, K. Kumagai, and Y. Iye, Phys. Rev. Lett. **70**, 2126 (1993).

<sup>14</sup>L. F. Mattheiss, Phys. Rev. B **6**, 4718 (1972).

<sup>15</sup>Y. Taguchi, Y. Tokura, T. Arima, and F. Inaba, Phys. Rev. B **48**, 511 (1993).

<sup>16</sup>Y. Tokura, J. Phys. Chem. Solids **53**, 1619 (1992).

<sup>17</sup>Preliminary results were reported by K. Kumagai, K.

Kawano, T. Suzuki, H. Takahashi, M. Kasuya, Y. Fujisima, Y. Taguchi, Y. Okada, and Y. Tokura, Physics B **186-188**, 1030 (1993).

<sup>18</sup>D. B. McWhan, J. P. Remeika, T. M. Rice, W. F. Brinkmann, J. P. Maita, and A. Menth, Phys. Rev. Lett. **27**, 941 (1971); D. B. McWhan, J. P. Remeika, J. P. Maita, H. Okinaka, K. Kosuge, and S. Kachi, Phys. Rev. B **7**, 326 (1973).

<sup>19</sup>D. A. Crandles, T. Timusk, J. D. Garrett, and J. E. Greedan, Physica C **201**, 407 (1992).

<sup>20</sup>N. Berk and J. R. Schrieffer, Phys. Rev. Lett. **17**, 433 (1966); S. Doniach and S. Engelsberg, *ibid.* **17**, 750 (1966).

<sup>21</sup>W. F. Brinkmann and T. M. Rice, Phys. Rev. B **2**, 4302 (1970).

<sup>22</sup>K. Kadowaki and S. B. Woods, Solid State Commun. **58**, 507 (1986).

<sup>23</sup>N. Kawakami and S. K. Yang, Phys. Rev. Lett. **65**, 2309 (1990).

<sup>24</sup>N. Furukawa and M. Imada, J. Phys. Soc. Jpn. **60**, 3604 (1991); **61**, 3331 (1992).

<sup>25</sup>F. Ohkawa, J. Phys. Soc. Jpn. **61**, 1615 (1992).

<sup>26</sup>R. M. White, *Quantum Theory of Magnetism* (McGraw-Hill, New York, 1970).

<sup>27</sup>D. C. McCollum, Jr. and J. Callaway, Phys. Rev. Lett. **9**, 376 (1962).

<sup>28</sup>G. G. Low, Proc. Phys. Soc. London **82**, 992 (1963).

<sup>29</sup>K. Kumagai, Y. Nakamura, I. Watanabe, Y. Nakamichi, and H. Nakajima, J. Magn. Magn. Mater. **76&77**, 601 (1988).

<sup>30</sup>N. Wada, H. Muro-oka, Y. Nakamura, and K. Kumagai, Physica C **157**, 453 (1989).

<sup>31</sup>N. Wada, T. Obana, Y. Nakamura, and K. Kumagai, Physica B **165-166**, 1341 (1990).

<sup>32</sup>H. Takagi, T. Ido, S. Ishibashi, M. Uota, and S. Uchida, *Phys. Rev. B* **40**, 2254 (1989).

<sup>33</sup>M. Sera, S. Shamoto, and M. Sato, *Solid State Commun.* **72**, 749 (1989).

<sup>34</sup>A. Iwai, M. Abe, H. Nakajima, and K. Kumagai, *Physica C*

**185-189**, 1349 (1991).

<sup>35</sup>Y. Yamada, K. Kakurai, Y. Endoh, T. R. Thurston, M. A. Kastner, R. J. Birgeneau, G. Shirane, Y. Hidaka, and T. Murakami, *Phys. Rev. B* **40**, 4557 (1989).